INSTITUTE OF PHYSICS PUBLISHING JOURNAL OF PHYSICS: CONDENSED MATTER

J. Phys.: Condens. Matter **17** (2005) 6575–6586 doi:10.1088/0953-8984/17/41/026

Spectroscopic and computer modelling studies of mixed-cation superionic fluorites

T T Netshisaulu[1,2], A V Chadwick[3], P E Ngoepe[2,4] and C R A Catlow[5]

[1] UNIFY Project, University of Limpopo, Turfloop Campus, P/Bag X1106, Sovenga, 0727, South Africa
[2] Materials Modelling Centre, University of Limpopo, Turfloop Campus, P/Bag X1106, Sovenga, 0727, South Africa
[3] School of Physical Sciences, University of Kent, Canterbury CT2 7NH, UK
[4] Division of Materials Science and Technology, CSIR, Pretoria 0001, South Africa
[5] Royal Institution of Great Britain, 21 Albermarle Street, London W1X 4BS, UK

Received 27 October 2004, in final form 4 August 2005
Published 30 September 2005
Online at stacks.iop.org/JPhysCM/17/6575

Abstract

Mixed-cation superionic fluorites are exceptionally good F^- ion conductors due to the mixed nature of the cation sublattice. In this study, we have used extended x-ray absorption fine structure (EXAFS) spectroscopy to gain insights into the local environments of the Cd and Pb cations (as a function of composition and temperature) in $CdF_2(xPbF_2)$ mixed-cation superionic fluorites. A high degree of disorder is shown around both cations. However, the extent of disorder is even larger around the Pb^{2+} in the entire series of solid solutions, with the highest disorder noted for the $x = 60$ mol% PbF_2 sample. The large values of the Debye–Waller factors of the Pb–F interactions are consistent with the low amplitudes of their Fourier transforms. This can be correlated with relative ionic conductivities of each composition in these materials. Molecular dynamics (MD) has been used as a complementary technique on structural properties; systems were modelled at temperatures ranging from liquid nitrogen temperature, 77 K, to 300 K. Our MD results confirm that disorder is greatest at concentrations $x \approx 60$ mol% PbF_2.

(Some figures in this article are in colour only in the electronic version)

1. Introduction

Mixed-cation superionic fluorite-structured systems, such as rubidium bismuth fluorites ($RbBiF_4$) and lead tin fluorites ($PbSnF_4$), have received considerable attention due to both the interest in the exceptionally high ionic conductivity (i.e. $\sigma \sim 10^{-3}\ \Omega^{-1}\ cm^{-1}$ at 100 °C) and the technological applications (e.g. fuel cells, gas sensors, use as electrolytes in light-weight batteries, etc). However, the high levels of disorder within these materials make it

difficult to obtain detailed information on them from experiment. Hence, the combined use of spectroscopic experiments together with computational approaches has been regarded as a solution to the problem.

EXAFS is an extremely powerful probe of local structure (up to 5–10 Å) around the cation sites in disordered materials. Previous EXAFS work on mixed-cation superionic fluorites with very high F^- ion conductivities successfully revealed the local structural environments of the cations in $RbBiF_4$ and $PbSnF_4$ [1–3]. The Fourier transform (FT) profiles obtained for the Rb and Bi edges in $RbBiF_4$ mixed systems showed the local ordering about Bi^{3+} to be much greater than about Rb^+. In addition, in the case of Bi no change in the amplitude of the first peaks was observed whilst the Rb edge EXAFS displayed a marked reduction in amplitude with an increase in temperature. This phenomenon is linked to an increase in the static component of the Debye–Waller factor in the neighbouring shell of Rb^+. The reduction in amplitude of the high-frequency components for Rb at high temperature is accounted for by a decrease in the Rb–F distance. Furthermore, the Rb–F bond length is marginally greater than the Bi–F bond length in these materials. On this basis, it was concluded that the Bi ions 'dictate' the structure by drawing F^- ions to form a tight coordination shell at a short distance which leaves the Rb–F shell comparatively disordered [1]. Further evidence to the observations above was that F^- ion vacancies were preferentially located in anion sites neighbouring cations having larger ionic radii and lower charges. This intriguing behaviour was attributed to the fact that it is electrostatically easy to remove F^- ions from lattice sites in excess of singly charged ions (e.g. Rb in $RbBiF_4$) (since Rb ions carry a lower charge of +1 as opposed to +3 for Bi ions) than to remove them from sites adjacent to the more highly charged Bi ions. However, there is considerable interest in synthesizing new materials with high ionic conductivity at lower operating temperatures.

In the present investigation, Cd and Pb cations in $CdF_2(xPbF_2)$ mixed-cation superionic fluorites have the same charge (+2) as in $PbSnF_4$ [2] so that no electrostatic advantage exists for the creation of F^- vacancies in anion sites adjacent to the cations with an excess of either Cd or Pb ions. Effects observed on the Sn edge in $PbSnF_4$ are similar to those observed on the Bi edge in $RbBiF_4$. On the other hand, for the Pb edge, effects observed are similar to those observed on the Rb edge. Furthermore, the Sn–F distances are shorter than the Pb–F distances. On the basis of this discussion, Cox *et al* [3] proposed that Rb^+ and Pb^{2+} ions transfer F^- ions from normal to interstitial sites with the creation of supplementary vacancies in the normal anionic sublattice, whilst Bi and Sn cations maintain a temperature-independent local environment.

The effects of disorder on the fluorine sublattice in $CdF_2(xPbF_2)$ were observed by Kosacki and co-workers [4] in the temperature dependence of the lattice constant. For pure PbF_2 crystals, deviation from linear dependence at temperatures above 600 K was noted. At these temperatures, specific heat anomalies were also observed. For $CdF_2(xPbF_2)$ mixed systems, the anomalies in the temperature dependence of the lattice parameter shift towards lower temperatures due to a decrease in the temperature of transition to the fast-ion phase. Furthermore, a correlation was found between the specific heat and the lattice constant anomalies. Kosacki *et al* [4] also noted that as the Pb content in the $CdF_2(xPbF_2)$ mixed-cation superionic fluorites was changed, a non-linear compositional dependence of the transition temperature T_c was observed which for $x = 60$ mol% PbF_2 attained a minimum at $T_c = 485$ K. However, a detailed study of the structural and transport properties of $CdF_2(xPbF_2)$ mixed systems in the whole compositional range has not been reported. Hence, the aim of this work is to examine the local environments of the ions, Cd^{2+} and Pb^{2+}, and to determine the extent of structural disorder using a combination of experiment and computer modelling techniques.

2. Experimental details

2.1. Preparation of materials

$CdF_2(xPbF_2)$ crystals with $x = 0$, 20, 40, 60, 80 and 100 mol% PbF_2 were prepared for this study in the Chemical Laboratory of the University of Kent, at Canterbury, in the UK. These specimens were finely ground (<20 μm) with a mortar and pestle, well diluted with boron nitride, and pressed under vacuum (10^{-6} Torr) into thin coherent pellets (200–400 μm thickness) using a 13 mm die. After preparation the samples were mounted in an evacuable crystal-heating furnace with beryllium windows.

2.2. Experimental procedure

EXAFS measurements around the Cd-K edge (26.716 keV) and the Pb-L_3 edge (13.036 keV) were carried out using the Science and Engineering Research Council's Synchrotron Radiation Source (SRS) facility on station 7.1 at Daresbury Laboratory, UK. The samples of $CdF_2(xPbF_2)$ ($x = 0$–100 mol% PbF_2) were mounted in an evacuable heating furnace with beryllium windows. The EXAFS absorption spectra were recorded at 77 and 300 K in the transmission mode using a double Si(111) crystal monochromator to study the L_3 absorption edge of Pb and the Si(220) one for the Cd edge. During the data collection, the SRS was operated at an electron energy of 2.0 GeV with a typical beam current of about 150 mA. Order-sorting monochromators were used to minimize harmonic contamination of the beam. Then, data were analysed using the EXAFS data reduction suite of programmes available at Daresbury Laboratory, namely EXCALIB, EXBACK and EXCURV98 [5].

The expected experimental errors for the radial distances are ± 0.01 Å, and the Debye–Waller (DW) factors ($2\sigma^2$) are normally good to $\pm 20\%$.

3. Computational details

The simulations in this study were carried out with the short-range interactions modelled by a standard rigid-ion potential model of the Buckingham form:

$$\Phi(r_{ij}) = A_{ij} \exp\left[\frac{-r_{ij}}{\rho_{ij}}\right] - \frac{C_{ij}}{r_{ij}^6} \tag{1}$$

where r_{ij} is the interionic separation, $A_{ij}\exp(-r_{ij}/\rho_{ij})$ denotes a repulsion when two neighbouring electron clouds overlap and C_{ij}/r_{ij}^6 represents a van der Waals attraction for F^-–F^- pairs.

The rigid-ion potential model takes no account of ionic polarizability, which can have an important influence on the dielectric properties. Provided the empirical approach is used, one can adjust a rigid-ion potential to reproduce at least the static dielectric properties [12]. In this study, the interionic potentials of CdF_2 and PbF_2 were derived simultaneously by empirically fitting to observed crystal properties, in particular the static dielectric constants (ε_o), where they were adjusted via a least squares fitting procedure. This process was repeated until an optimal agreement between the calculated and experimental properties was obtained. Table 1 lists a common set of derived interionic potentials used in this study. It is worth noting that previous MD simulations, in particular, a recent shell model MD study on CaF_2, found that rigid-ion potential parameters are adequate for the calculations of structural and transport properties in superionic conductors [6, 7].

The MD technique was used to study the structure and ion motion both on the cation and anion sublattices in $CdF_2(xPbF_2)$ mixed crystals using the DLPOLY code [8]. Simulation runs

Table 1. Derived short-range interatomic potential parameters for the $CdF_2(x$ mol% $PbF_2)$ mixed-cation superionic fluorites. (Note: cut off = 12 Å.)

Interaction	A_{ij} (eV)	ρ_{ij} (Å)	C_{ij} (eV Å^{-6})
Cd^{2+}–F^-	420.060	0.3529	0.0280
Pb^{2+}–F^-	157.339	0.4662	0.9284
F^-–F^-	160 919.850	0.1758	22.3070

were started from the fluorite structure, where a simulation box containing 768 particles (256 cations and 512 anions) was set up. Periodic boundary conditions were applied to eliminate the effects of the surface, and the ensemble used imposes the conditions of constant temperature and volume (*NVT*).

For each doped sample x, a suitable number of Cd^{2+} ions were replaced by Pb^{2+} ions at random. Then, each system was allowed to evolve in time. After each time-step (δt) of 10^{-15} s, positions and velocities of each ion were updated using the procedures based on Newton's equations of motion. Equilibration (i.e. the periodical scaling of velocities to keep the simulation at a specified temperature, where $T = 77, 300$ and 700 K in the present study) for each simulation was attained after a period of at least 3000 δt ($\approx$3 ps; ps $= 10^{-12}$ s), followed by a simulation run for about 50 000 δt ($\approx$50 ps). This period was sufficiently long for noting a diffusion process in $CdF_2(x PbF_2)$. A wealth of information on structural (in particular, the radial distribution functions (RDFs)) and transport properties may be obtained from the subsequent data. The simulations were run on Silicon Graphics servers at the University of Limpopo, in the Materials Modelling Centre.

4. Results and discussion

In this study, it is useful to consider what changes occur in the structural and transport properties of $CdF_2(x PbF_2)$ mixed crystals as the composition is varied. Figures 1(a) and (b) compare the first peaks in the FTs (determined from EXAFS) and the RDFs (obtained from MD calculations) for the Cd–F interactions in $CdF_2(x PbF_2)$ mixed-cation superionic fluorites at $T = 77$ K. In each case, the effect of composition x on the FTs and the RDFs, respectively, has been monitored.

Figure 1(a) shows that as the value of x is increased in the composition range $0 < x < 60$ mol% PbF_2, a decrease in the amplitude of the FTs is observed. For $60 < x < 100$ mol% PbF_2, a rise in the FTs is seen. In addition, a broadening of the profile is observed with an increase in PbF_2 content, although the centre of the peak does not change. Comparing the shapes of the curves in figures 1(a) and (b), it is seen that the calculated RDF curves qualitatively reproduce the pattern of the experimentally observed features. It is also interesting to note from figures 1(a) and (b) that both techniques reveal a minimum in the curve for the $x = 60$ mol% PbF_2 sample. However, the experimental profiles are broader and less pronounced than those in the calculations. The explanation could be the failure of the rigid-ion model to account for polarization effects (which were neglected in the calculations) in these mixed materials.

Similarly, figures 2(a) and (b) show the composition dependence of the Pb–F FTs and RDFs, respectively, for the various samples in $CdF_2(x PbF_2)$ mixed crystals. The Pb–F profiles vary with concentration x in a similar fashion as for the Cd–F profiles. Thus the amplitudes of the FTs/RDFs decrease with increase in concentration x and the minimum curve occurs at $x = 60$ mol% PbF_2. As a result, the present results indicate that doping increases the disorder

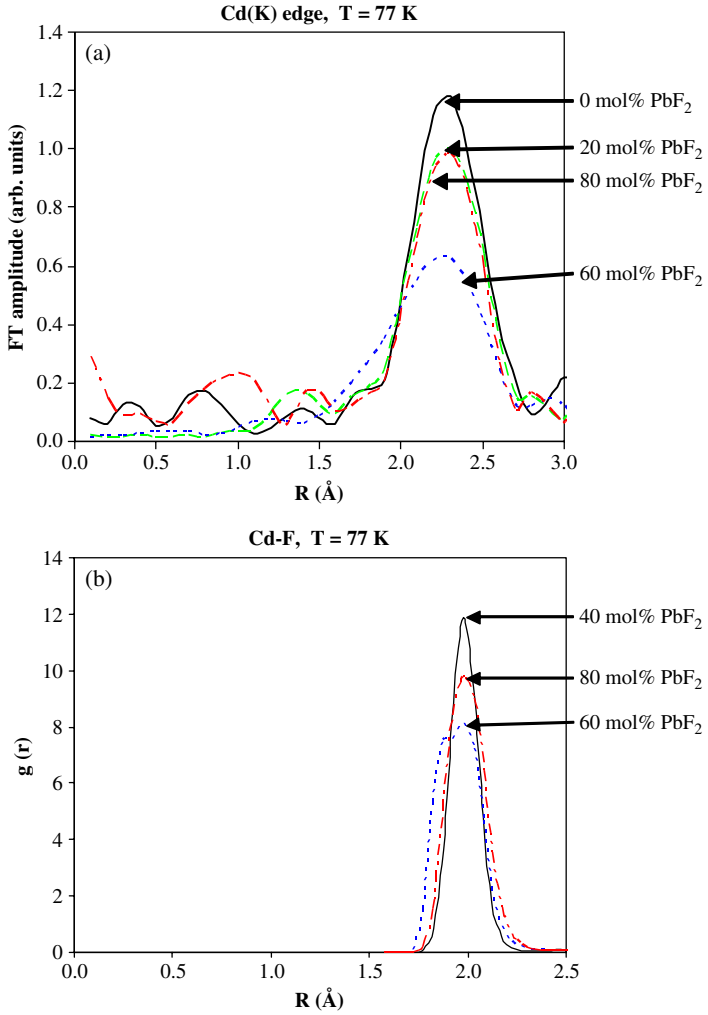

Figure 1. The concentration dependence of the (a) Cd edge Fourier transform and (b) calculated RDFs for Cd–F at $T = 77$ K in $CdF_2(xPbF_2)$ crystals. In (b), the Cd–F peak for the $x = 0$ mol% sample has been left out for clarity purposes since it is far greater than the peaks for other concentrations from calculations.

around both cations (i.e. Cd^{2+} and Pb^{2+} ions) until concentration $x = 60$ mol% PbF_2 is reached. There is, however, an important difference, namely, the Pb–F profiles are systematically broader and lower in amplitude than those for the Cd–F across the entire composition. This suggests that static disorder is predominant around the Pb cations in the entire composition range.

The diffusion coefficients (D_i) can be obtained from the Einstein relationship:

$$6D_i = \lim_{\Delta t \to \infty} \frac{\left[\langle r_i(\Delta t)^2\rangle - B_i\right]}{\Delta t} \tag{2}$$

where B_i is the thermal factor arising from atomic vibrations. However, as indicated, the relationship strictly holds only in the limit as $\Delta t \to \infty$.

Figure 3(a) shows that diffusion of F^- ions is negligible at temperature $T = 300$ K, and becomes evident for the dopant range 40 mol% $\leqslant x \leqslant$ 100 mol% PbF_2 at $T = 700$ K.

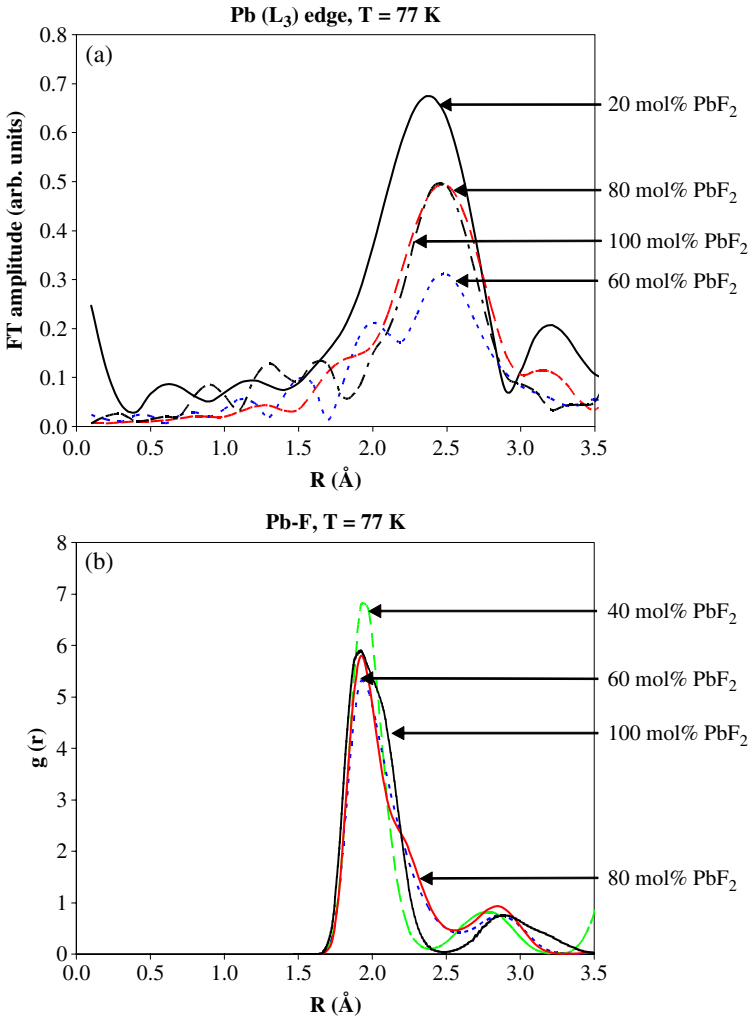

Figure 2. The concentration dependence of the (a) Pb edge Fourier transform and (b) calculated RDFs for Pb–F at $T = 77$ K in $CdF_2(x PbF_2)$ crystals.

A striking feature is that the highest value of diffusion is observed on the anion sublattice at the composition $x = 60$ mol% PbF_2, followed by a decrease after the maximum. However, for lower dopant range 0 mol% $\leqslant x \leqslant$ 20 mol% PbF_2, no fast-ion conduction is predicted at $T = 700$ K, indicated by a constant variation of mean-square displacements with time Δt (see figure 3(b)). This observation indicates that the transition temperatures for samples $x = 0$ mol% PbF_2 and $x = 20$ mol% PbF_2 are well above $T = 700$ K, a result which is consistent with our previous observation on the transition temperature (T_c) from a non-conducting to a conducting state of pure CdF_2 [9]. Hence, substantial fluorine diffusion in mixed-cation superionic fluorites takes place below the transition temperature of pure CdF_2, which is about 1000 K. In contrast, cations (both Pb^{2+} and Cd^{2+} ion species) do not contribute to diffusion even at 700 K (not shown here) in all samples, indicating that the simulated material is below its melting point. A similar behaviour was noted in oxygen [10] and fluorine-ion conductors [11, 12] from MD studies. Hence, the fluorite structure is maintained as the system

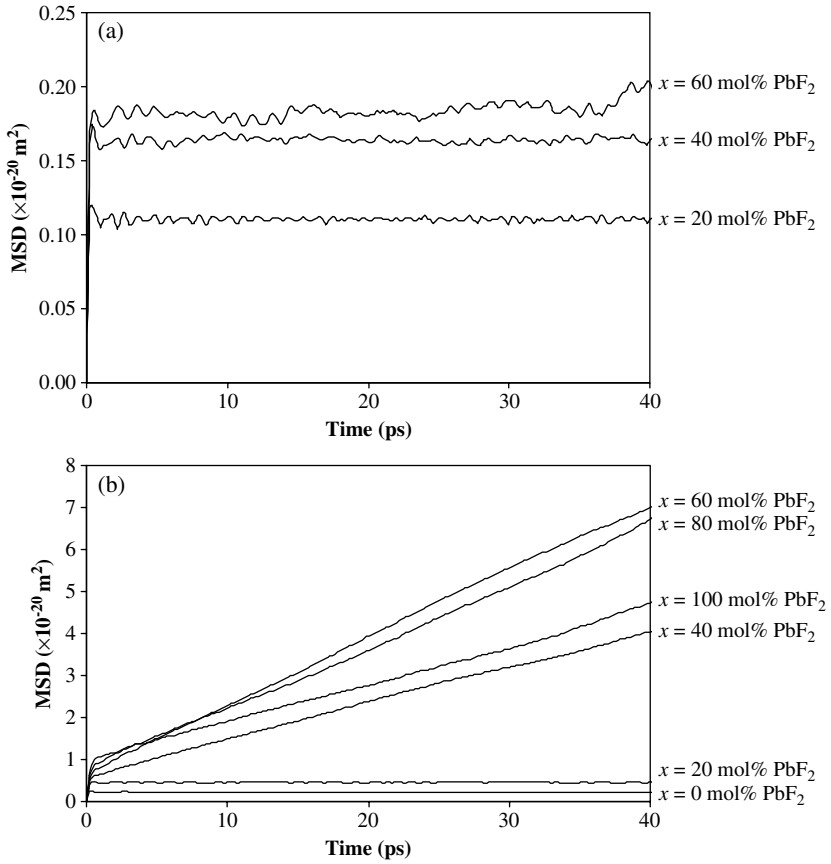

Figure 3. Mean-square displacements of fluorine ions in various concentrations of PbF_2 in $CdF_2(xPbF_2)$ at temperatures (a) $T = 300$ K and (b) $T = 700$ K.

evolves from CdF_2 to PbF_2, with the role of the cation sublattice being to maintain long-range order of the materials.

From the diffusion coefficients it is possible to use the Nernst–Einstein approximation to determine the conductivity (σ):

$$\sigma = \frac{n}{f_T}\left[\frac{D_t q^2}{kT}\right] \tag{3}$$

where n is the number of mobile species per unit volume (cm^{-3}), f is a correlation factor and it is characteristic of the lattice geometry (for fluorite lattices in an anion sublattice where the interstitialcy non-collinear mechanism takes place its exact value is $0.9855 \approx 1$, which is reasonable given the other approximations), q is the charge in Coulombs (C), k is the Boltzmann constant in J K^{-1}, T is the temperature in kelvin (K), and D_t is the tracer diffusion coefficient in cm^2 s^{-1}.

The derived transport coefficients from the simulations are given in table 2 at $T = 300$ and 700 K.

The dependence of the ionic conductivity on several compositions x of $CdF_2(xPbF_2)$ mixed-cation superionic fluorites obtained from MD calculations is shown both in table 2 and in figure 4(a). The corresponding composition dependence of the activation energies is

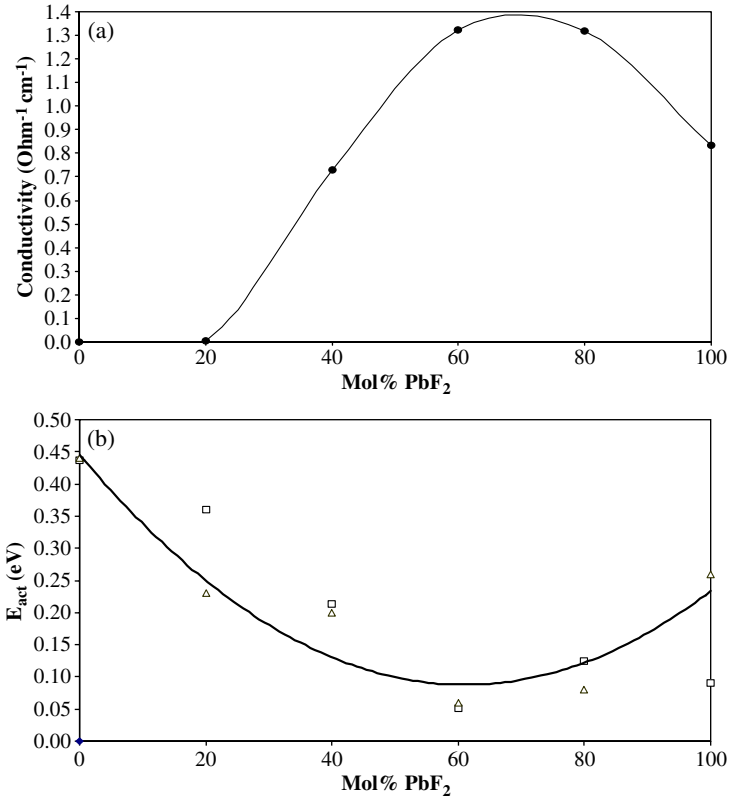

Figure 4. Composition dependence of the (a) ionic conductivity at $T = 700$ K and (b) activation energy E_{act} in $CdF_2(x PbF_2)$ systems. □: present work; Δ: experimental data from Kosacki *et al* [4]. The curved line is not a fit, but a guide to the eye.

presented in figure 4(b) (squares). The curve in figure 4(a) is characterized by a maximum in ionic conductivity for $x \approx 60$ mol% PbF_2. The results also show that the ionic conductivity markedly decreases after the maximum. In essence, such an evolution of the ionic conductivity within these systems can readily be explained by similar arguments to those advanced by Cox *et al* in their detailed computer simulation studies on transport properties of analogous materials (e.g. $RbBiF_4$) [2]. As the Pb concentration x approaches 60 mol% PbF_2, migration of F^- ions (from lattice positions) into interstitial ones increases, since F^- ions are easily transferred into interstitial sites adjacent to a local excess of Pb^{2+}. This process leads to the creation of supplementary vacancies in the anionic lattice positions. However, for concentrations beyond $x \approx 60$ mol% PbF_2, the migration of F^- ions into interstitial sites from lattice positions decreases leading to a decrease in diffusion coefficients. The maximum in ionic conductivity corresponds to a minimum (dip) in the activation energy (see figure 4(b)). In figure 4(b), the trend of the calculated activation energies is compared with the one obtained from experiments by Kosacki and co-workers [4]. These results are satisfactory in that they compare reasonably well although the scatter is large at low and high dopant concentrations. Relatively low values of the activation energy of conductivity for the mixed crystal at $x \approx 60$ mol% PbF_2 clearly suggests a rapid increase in mobility of F^- ions through the bulk—a feature that is in line with the minimum curve in the FTs/RDFs. These results clearly show the complementary

Table 2. Transport coefficients for F^- ions in specimens (a) $x = 0$–40 mol% PbF_2 and (b) $x = 60$–100 mol% PbF_2 mixed-cation superionic fluorites.

(a)	Composition x (mol% PbF_2)					
	0		20		40	
T (K)	D_{calc} ($cm^2\ s^{-1}$)	σ_{calc} ($\Omega^{-1}\ cm^{-1}$)	D_{calc} ($cm^2\ s^{-1}$)	σ_{calc} ($\Omega^{-1}\ cm^{-1}$)	D_{calc} ($cm^2\ s^{-1}$)	σ_{calc} ($\Omega^{-1}\ cm^{-1}$)
300	6.45×10^{-10}	7.726×10^{-4}	1.03×10^{-9}	1.234×10^{-3}	1.43×10^{-8}	0.017
700	1.40×10^{-9}	8.384×10^{-4}	4.97×10^{-9}	2.551×10^{-3}	1.42×10^{-6}	0.729
(b)						
	60		80		100	
T (K)	D_{calc} ($cm^2\ s^{-1}$)	σ_{calc} ($\Omega^{-1}\ cm^{-1}$)	D_{calc} ($cm^2\ s^{-1}$)	σ_{calc} ($\Omega^{-1}\ cm^{-1}$)	D_{calc} ($cm^2\ s^{-1}$)	σ_{calc} ($\Omega^{-1}\ cm^{-1}$)
300	1.81×10^{-8}	0.022	7.03×10^{-8}	0.084	2.06×10^{-7}	0.025
700	2.58×10^{-6}	1.324	2.57×10^{-6}	1.319	1.62×10^{-6}	0.832

Table 3. Structural parameters obtained from EXAFS data of $CdF_2(xPbF_2)$ mixed solutions for the first F^- shell as a function of composition and temperature for (a) Cd edge and (b) Pb edge.

(a)	Composition x (mol% PbF_2)									
	0		20		40		60		80	
T (K)	R (Å)	σ^2 (Å^2)	R (Å)	σ^2 (Å^2)	R (Å)	σ^2 (Å^2)	R (Å)	σ^2 (Å^2)	R (Å)	σ^2 (Å^2)
77	2.310	0.012	2.294	0.014	2.259	0.025	2.275	0.027	2.296	0.016
300	2.295 2.33[a]	0.020	2.293	0.021	—	—	2.249	0.025	2.288	0.021
(b)										
	20		40		60		80		100	
T (K)	R (Å)	σ^2 (Å^2)	R (Å)	σ^2 (Å^2)	R (Å)	σ^2 (Å^2)	R (Å)	σ^2 (Å^2)	R (Å)	σ^2 (Å^2)
77	2.485	0.023	2.480	0.027	2.496	0.042	2.524	0.028	2.524	0.027
300	—	—	2.406	0.049	2.438	0.048	2.484	0.063	2.500 2.57[b]	0.049

[a] X-ray diffraction results for pure CdF_2.
[b] X-ray diffraction results for pure PbF_2

nature of the EXAFS and MD techniques. Similar dependences of both ionic conductivity and activation energies on composition in related solid solutions such as $RbBiF_4$, were also observed by Catlow and co-workers [1].

Table 3 gives the structural parameters (radial distances and $2\sigma^2$) determined from the first peaks of the FTs for both Cd-K and Pb-L_3 edges in $CdF_2(xPbF_2)$. Inspection of the table shows that the Pb–F Debye Waller factors ($2\sigma^2$) are larger than for Cd–F, showing even larger static disorder about Pb. Furthermore, the Pb–F distances are consistently larger than Cd–F distances, again reflecting the high state of disorder on the Pb sites. Hence, the neighbourhoods of the Cd and Pb ions are different.

Figures 5 and 6 display the Cd–F and Pb–F FTs/RDFs for $CdF_2(xPbF_2)$ at temperatures of 77 and 300 K. As expected, there is a marked loss in amplitude of both Cd–F and Pb–F peaks as

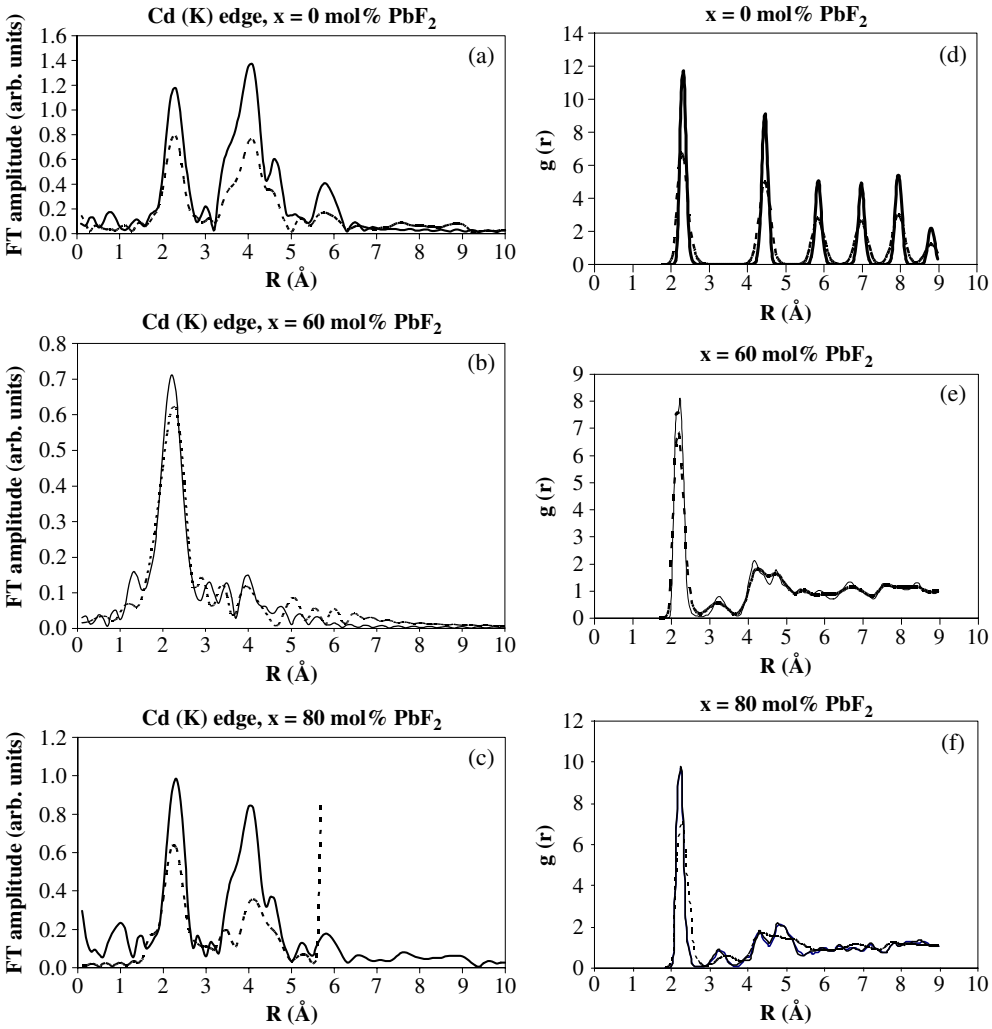

Figure 5. Temperature dependence of the ((a)–(c)) Cd edge Fourier Transforms and the ((d)–(f)) calculated radial distribution functions for Cd–F at various concentrations x in $CdF_2(xPbF_2)$. Full curve: $T = 77$ K; broken curve: $T = 300$ K.

we go from 77 to 300 K. This behaviour is analogous to the effects observed on the Rb and Pb edges in $RbBiF_4$ and $PbSnF_4$, respectively, and the amplitude reduction is similarly consistent with a large increase in the Debye–Waller factors. For both Cd–F and Pb–F peaks, there is good agreement between experimental and computational results and minor discrepancies are probable within the errors of the experimental results and the uncertainties in the calculations attributable to the quality of the interionic potentials used.

5. Conclusions

We have studied the structural and dynamical properties of the mixed-cation superionic fluorite $CdF_2(xPbF_2)$ for a series of dopant concentrations. A qualitative picture of the ionic conductivity variation with content has been presented from MD calculations. The

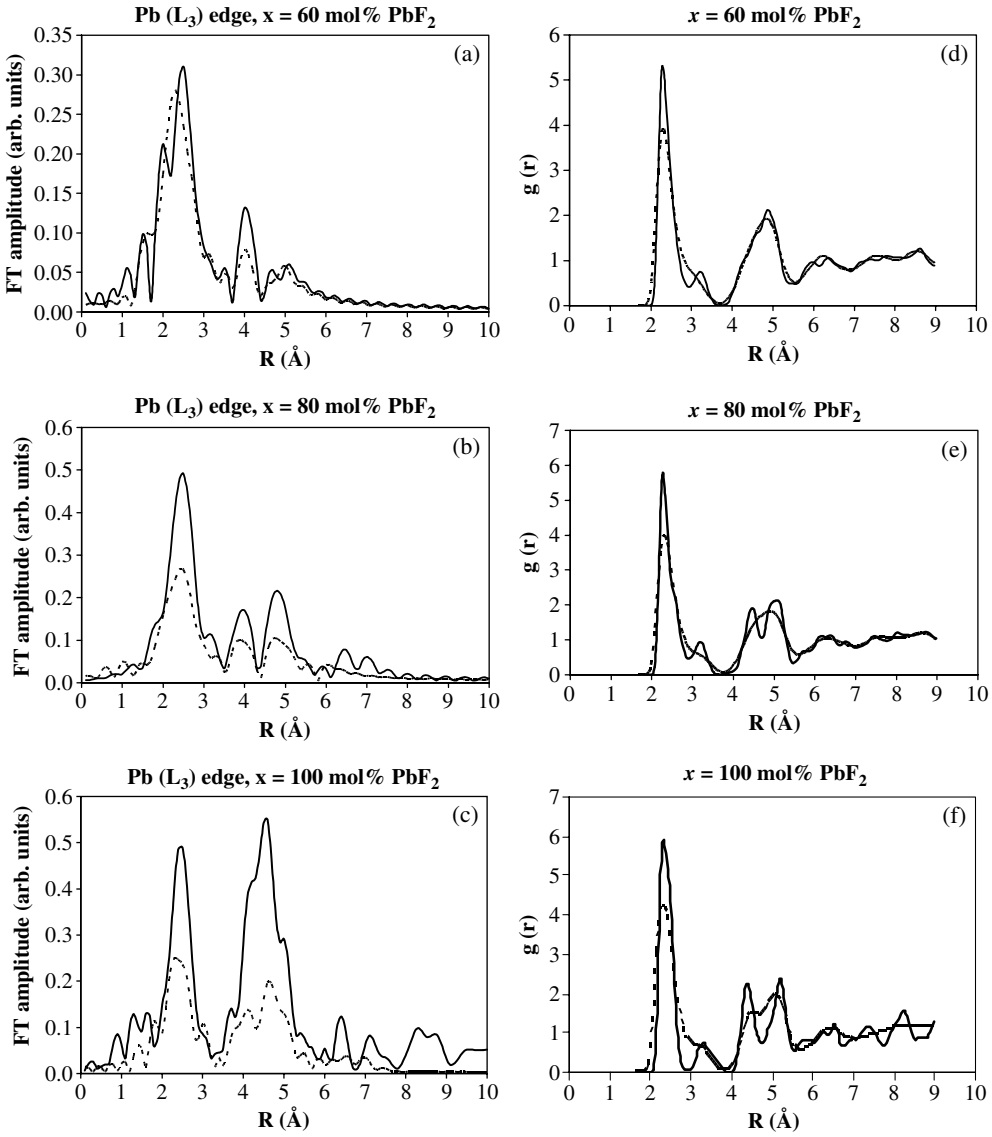

Figure 6. Temperature dependence of the ((a)–(c)) Pb edge Fourier transforms and the ((d)–(f)) calculated temperature dependence of the Pb–F radial distribution functions at various concentrations x in $CdF_2(x PbF_2)$. Full curve: $T = 77$ K; broken curve: $T = 300$ K.

exceptional ionic conductivity in these systems is explained by attributing it to the ease with which F^- ions may occupy interstitial positions in the vicinity of Pb^{2+} ions which possess higher polarizability. The role of Cd^{2+} ions is to provide the immobile 'lattice' through which the mobile assembly of F^- ions can migrate. The structure in the simulation was verified by the calculation of the radial distribution functions which were compared with the FTs obtained from EXAFS. Significantly greater disorder is noted around the Pb^{2+} ions in comparison with the Cd^{2+} ions. In addition, the two techniques have revealed clear evidence that CdF_2 samples doped with 60 mol% PbF_2 crystals exhibit the best fast-ionic properties compared with those

of other concentrations. Hence, this class of materials is quite suitable for applications in all-solid batteries and the study opens up more avenues for the development/synthesis of new electrolytes in micro-batteries with enhanced ionic conductivities, even at low temperatures.

Acknowledgments

We are grateful to the Science and Engineering Research Council and staff of Daresbury Laboratory for the provision of synchrotron radiation and associated facilities, and to the NRF/Royal Society Initiative for financial support.

References

[1] Catlow C R A, Chadwick A V, Greaves G N and Moroney L M 1985 *Cryst. Lattice Defects Amorphous Mater.* **12** 193
[2] Cox P A, Catlow C R A and Chadwick A V 1994 *J. Mater. Sci.* **29** 2725
[3] Catlow C R A, Cox P A, Jackson R A, Parker S C, Price G D, Tomlinson S M and Vetrivel R 1989 *Mol. Simul.* **3** 49
[4] Kosacki I, Litvinchuk A P, Tarasov J J and Valakh M Ya 1989 *J. Phys.: Condens. Matter* **1** 929
[5] Binsted N, Campbell J N, Gurman S J and Stephenson P C 1992 *SERC Daresbury Program Library Daresbury Laboratory* Warrington, Ceshire WA4 4AD, UK
Binsted N 1998 *EXCURV98: CCLRC Daresbury Laboratory Computer Program*
[6] Gillan M J 1985 *Physica* B **131** 157
[7] Lindan P J D and Gillan M J 1993 *J. Phys.: Condens. Matter* **5** 1019
[8] Smith W and Forester T R 1996 DLPOLY 2.0: A general purpose parallel molecular dynamics simulation package *J. Mol. Graphics* **14** 136
[9] Netshisaulu T T 1996 *MSc Thesis* University of the North, Republic of South Africa
[10] Li X and Hafskjold B 1995 *J. Phys.: Condens. Matter* **7** 1255
[11] Netshisaulu T T, Ngoepe P E and Chadwick A V 1999 *Mol. Simul.* **22** 1
[12] Dent A, Madden P A and Wilson M 2004 *Solid State Ion.* **167** 73